Particuology 36 (2018) 158–164

Contents lists available at ScienceDirect

Particuology

journal homepage: www.elsevier.com/locate/partic

Nitrogen release characteristics of polyethylene-coated controlled-release fertilizers and their dependence on membrane pore structure

Xiangdong Yang[a,b,*], Rongfeng Jiang[b], Yangzheng Lin[c], Yanting Li[a], Juan Li[a], Bingqiang Zhao[a]

[a] Key Laboratory of Plant Nutrition and Fertilizer, Ministry of Agriculture/Institute of Agricultural Resources and Regional Planning, Chinese Academy of Agricultural Sciences, Beijing 100081, China
[b] College of Resources and Environmental Sciences, Centre for Resources, Environment and Food Security, China Agricultural University, Beijing 100193, China
[c] Geophysical Laboratory, Carnegie Institution of Washington, Washington, DC 20015, USA

ARTICLE INFO

Article history:
Received 11 October 2016
Received in revised form 8 May 2017
Accepted 18 May 2017
Available online 29 July 2017

Keywords:
Controlled-release fertilizer
Nutrient release period
Membrane pore structure
Mercury porosimetry
Pore size

ABSTRACT

In this study, controlled-release fertilizers (CRFs) with five different nitrogen release periods were prepared by coating large urea particles with polyethylene (PE) membranes under various experimental conditions. The preliminary and differential solubility rates, release periods, and membrane pore sizes of the obtained CRFs were measured using water immersion, scanning electron microscopy, and mercury porosimetry. For all CRF samples, the median pore diameters of the membranes were equal to 4.5–5.3 nm and pores with sizes smaller than 10 nm accounted for 86–96% of the total pore surface area. The obtained pore diameter distributions differed for the five studied types of CRF, having release periods of 1, 2, 4, 6, and 8 months. Thus, for the CRFs with a 1-month release period, the maximum pore diameter reached a magnitude of 4000 nm, while this value did not exceed 30 nm for the CRFs with a release period of 8 months. Hence, we have established a relationship between the release period of CRFs and their effective maximum pore sizes.

Introduction

Controlled-release fertilizers (CRFs) can improve the nutrient use efficiency of plants by increasing their nutrient uptake, which decreases fertilization frequency and, therefore, substantially reduces the consumption of human resources and possible adverse effects on the environment (Chu, Hosen, & Yagi, 2007). Despite the relatively large number of CRFs utilized in agriculture, the mechanism of nutrient release through membranes and its related parameters have not been elucidated yet. Hence, various experimental methods have been developed to determine the CRFs' nutrient release rate in water and examine the pore structure characteristics of CRF membranes.

Immersion is a widely used method for estimating the time-dependent volume of nutrients that have been previously released into water or soil by CRFs (Oertli & Lunt, 1962; Shaviv & Mikkelsen, 1993; Trenkel, 2010). As a result, the preliminary solubility rate, differential solubility rate, and release period of a fertilizer can be obtained from the volume-time relationship determined via a water immersion method (Fujita, 1996). These parameters reflect the functionality of the CRFs membrane, nutrient release characteristics, and the CRFs' applicability to a particular plant (Yang, Cao, Jiang, & Zhang, 2005). For example, Shavit, Reiss, and Shaviv (2003) studied the wetting mechanisms of gel-based CRFs using a controlled-release experimental device, which consisted of a glass tube and a porous plate. They concluded that the entire CRF release process could be divided into the following three stages: penetration of water vapor, nutrient dissolution, and nutrient release through a membrane (Shavit, Shaviv, & Zaslavsky, 1995; Shavit et al., 2003). Du, Zhou, Shaviv, and Wang (2004) used a mathematical model based on Fick's second diffusion law to describe the potassium release from a polymer-coated CRF and concluded that

* Corresponding author at: No. 12 Zhongguancun South St., Haidian District, Beijing, China. Fax: +86 10 82108664.
E-mail address: yangxiangdong@caas.cn (X. Yang).

http://dx.doi.org/10.1016/j.partic.2017.05.002

Nomenclature

$A_{<10}$	Cumulative surface area of pores with sizes less than 10 nm, %
D_A	Average pore diameter (4 V/A), nm
D_M	Median pore diameter, nm
J	Molar flux, mol/(m^2 s)
k	Conversion quotiety
K	Hindrance factor for diffusion
r	Average pore semi-diameter (8 V/A), nm
T	Release duration, day
V_T	Total intrusion volume, mL/g
ε	Porosity, %
$\eta_1, \eta_{\Delta t}, \eta_{28}$	Preliminary solubility rate, differential solubility rate, and cumulative solubility rate after 28 days

the release of nutrients was mainly affected by the diffusion coefficient, membrane thickness, and granule radius. Al-Zahrani (1999) studied various CRFs with spherical particles and found that their release characteristics depended on their fertilizer formulation. The mathematical models' formulation determined the release characteristics of CRFs.

The models utilized in the studies mentioned above were based on phenomenological equations describing the relationship between the permeation flux and chemical potential energy. They could explain some of the observed experimental phenomena but were unable to elucidate the relationship between the membrane structure and the transfer process (Mulder, 1996). The structure of membranes prepared by phase inversion is affected by many factors, such as the concentration of the utilized membrane liquid, solvent type, and additive type (Ma & McHugh, 2007; Siepmann, Siepmann, Walther, MacRae, & Bodmeier, 2008; Van de Witte, Dijkstra, Van den Berg, & Feijen, 1996). Sun, Huang, and Chang (1999) suggested that sprayed membranes were more porous than casted membranes; however, it was difficult for them to predict the type of membrane structure without performing experimental measurements. Scanning electron microscopy (SEM) is a popular technique that allows direct observation of the membrane morphology (Mulder, 1996). Nevertheless, SEM can provide only local and sectional information, and further image analysis is required to determine the distribution, quantity, and sizes of the membrane pores (Hernandez et al., 1997).

Bubble point testing, Brunauer–Emmett–Teller analysis, and mercury porosimetry (MP) are widely used techniques for determining the pore structure of industrial membranes. However, most of these methods are not applicable to studies of the controlled-release membranes formed on the surface of basal granules. In general, MP can be used to evaluate the performance of small particles (Calvo, Hernandez, Pradanos, Martınez, & Bowen, 1995; León y León, 1998; Liu, Du, Zhu, & Xu, 2007; Mohl & Winter, 2004) and thus estimate the pore size distribution of membranes fabricated by a spray phase inversion method since its measuring range spans from 0.36 to 420 mm. However, the use of MP to measure the pore size distribution of CRF membranes has not been reported in the literature.

SEM images of the surface and cross-sectional views were obtained to characterize the pores of the controlled-release membranes fabricated in this study and elucidate the relationship between the pore structure and the nutrient release performance. MP was used to evaluate the membrane pore size characteristics including the pore size distribution, specific surface area, porosity, and other parameters, while the water immersion method was used to determine the preliminary solubility rate, differential solubility rate, and CRF release duration. In total, the pore size distributions of five CRFs types were analyzed in detail to obtain the relationship between their release periods and pore diameters.

Experimental

Materials and equipment

Five different types of CRFs with release periods of 1, 2, 4, 6, and 8 months were prepared in this study. They were manufactured at the Department of Plant Nutrition of China Agricultural University by spraying the corresponding membrane solutions onto the surface of large urea particles with a fluidized-bed spray coater. The membrane solutions were prepared by dissolving low-density PE (LDPE) and wax reagents in ethylene tetrachloride (TCE) at 120 °C. The coated fertilizer with the mass ratio between different components of urea:LDPE:TCE:wax:dye = 100:8.0:160:1:0.01 was made by changing the concentration of membrane solutions and the spraying rate. PE (1F7B, 25 kg/bag) was purchased from China SINOPEC Yanshan Chemical Corporation. TCE (300 kg/barrel) was obtained from the Dow Chemical Company (United States). Wax (melting point: 60 °C, 25 kg/bag) was acquired from the Fushun Petrochemical Branch Company (China). Urea (40 kg/bag, particle size: 2–4 mm) was obtained from Hebei Cangzhou Dahua Co., Ltd. (China). Both pigment Paliotol® yellow K2270 and Heliogen® blue K6907 dyes (BASF, Germany) were used. The homemade fluidized-bed spray coater (capacity: 1.5 kg urea) utilized a BIMJ2022S303 spraying nozzle manufactured by Ikeuchi (Japan).

A UV-2201 ultraviolet–visible (UV–vis) spectrophotometer (Shimadzu, Japan), JSM-7401F scanning electron microscope (Jeol, Japan), an Autopore IV 9510 mercury porosimeter (Micromeritics, United States), and a PT120 electronic balance (Sartorius, Germany) were used. A biochemical incubator and an HPS-250 incubator with controlled humidity were manufactured by the Harbin Dongming Medical Instrument Factory (China).

Pore structure examination

The prepared CRFs were pretreated before their membrane pore structures were examined. About one eighth of the spherical membrane was cut from each studied CRF particle's surface using a section razor. For each CRF type, 100 membrane pieces were collected from 100 CRF particles and cleaned three times by de-ionized water followed by drying in a vacuum oven at a temperature of 40 °C for 12 h. The dried samples were directly used for SEM observations and MP measurements. Similar to the shortest stave in a bucket, the largest membrane pores were expected to affect the nutrient release rates significantly. The effective maximum pore diameters were determined for all the studied CRF types using the following procedure. First, the CRF samples were immersed in water for 24 h and dried. Next, small membrane pieces were cut from the dried fertilizer particles, leaving parts of the corresponding urea cores exposed. Finally, the maximum pore diameters of the cut membranes were measured using the bubble pressure method (Xu et al., 2016). The obtained maximum pore diameters were considered the effective maximum pore sizes of the membranes.

Nitrogen release characteristics

In this study, water immersion was used to investigate the parameters of the controlled release of nitrogen species by the CRFs. 100 g of the coated CRFs particles was packed in a nylon net bag and placed into a plastic bottle, which was filled with 200 mL of distilled water and covered. Afterward, the temperature of the bottle was maintained at 25 °C using a thermostat for static release. The released amount of nitrogen was determined

Table 1
Nitrogen release and membrane pore size characteristics of the studied controlled-release fertilizer samples.

Sample	η_1 (%)	η_{28} (%)	$\eta_{\Delta t}$ (%)	T (day)	V_T (mL/g)	D_A (nm)	D_M (nm)	ε (%)	$A_{<10}$ (%)	r^2 (nm^2)
1	5.6	76	2.607	30	0.168	95	5.3	51	86	2240
2	1.5	35	1.241	64	0.123	87	4.7	45	88	1880
3	0.7	18	0.641	125	0.115	79	4.5	36	88	1570
4	0.6	13	0.459	174	0.099	53	4.7	43	88	690
5	0.4	9	0.319	250	0.085	25	4.8	33	91	160

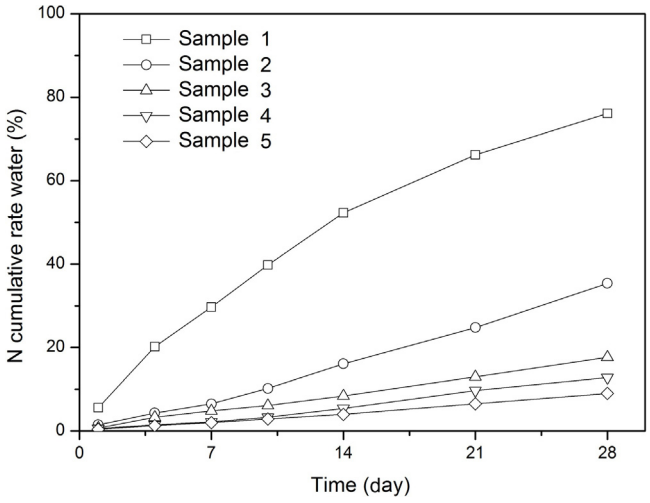

Fig. 1. Nutrient cumulative release plots for the five CRFs samples listed in Table 1.

by a *para*-dimethylaminobenzaldehyde-based spectrophotometric method after 1, 4, 7, 10, 14, 21, and 28 days. The bottle was refilled with pure water after each measurement to maintain a low concentration of the released nitrogen species.

The cumulative solubility rate of nitrogen was calculated by the following formula:

$$\eta_n = \frac{M_n}{M} \times 100\%, \quad (1)$$

where M is the total nitrogen content in the studied sample, and M_n is the amount of the released nitrogen after n days. The solubility rate η_1 measured after the first day was called the preliminary solubility rate. The differential solubility rate was calculated as follows:

$$\eta_{\Delta t} = \frac{\eta_n - \eta_1}{n-1}, \quad (2)$$

The corresponding release period could be estimated as

$$T = \frac{80\% - \eta_1}{\eta_{\Delta t}} + 1. \quad (3)$$

A fertilizer can be called CRFs if $\eta_1 < 15\%$, $0.25\% < \eta_{\Delta t} < 2.5\%$, and $T > 21$ (Trenkel, 2010).

Results and discussion

Osmotic characterization of CRFs membranes

The obtained cumulative solubility rates of nitrogen in water were linearly dependent on the corresponding release times for all five CRF types (see Fig. 1). The preliminary solubility rates, differential solubility rates, and release periods of these fertilizers, together with their pore characteristics, are listed in Table 1. The obtained results indicate that the preliminary solubility rates of all the coated CRFs are ~5.6–0.4% and the differential solubility rates are ~2.6–0.3% during release periods of 29–250 days; hence, all of them can be considered standard CRFs. The notations 1, 2, 3, 4, and 5 correspond to the CRF release periods of 1, 2, 4, 6, and 8 months, respectively.

SEM studies of membrane structures

The SEM membrane images obtained for the five types of PE-coated CRFs at a magnification of ×10,000 are shown in Fig. 2. The observed pores were distributed irregularly on the surfaces of the controlled-release membranes, and their sizes depended on the release periods of the corresponding CRF samples. Thus, sample 1 contained the largest pores, while the smallest pores (which were hardly observable by SEM) were detected in sample 5. The cross-sectional SEM image obtained for sample 1 (Fig. 2(a)) revealed that its inner membrane part was also porous.

Pore size distributions

The membrane pore size significantly affected the nitrogen release rate; thus, membranes with larger pores exhibited shorter release periods, while membranes with smaller pores had longer release periods. The pore size distributions determined via MP for the five studied types of membranes are presented in Table 1 and Fig. 3. The cumulative pore volume dramatically increased with decreasing membrane pore size below 25 nm (Fig. 3(a)). While samples 1, 2, and 3 contained fractions of pores with diameters larger than 100 nm, such large pores were not detected for samples 4 and 5, consistent with the SEM observations described in Fig. 2. Pores with diameters smaller than 10 nm constituted more than 86% of the total cumulative surface area (Table 1). The median membrane pore size was 4.5–5.3 nm (Table 1). This result is inconsistent with the above results obtained by using SEM, and the reason is that pores with diameters smaller than 10 nm could not be observed by SEM because the corresponding membrane structures were destroyed by the high temperature generated during the high-resolution scanning process. As a result, only magnifications below ×50,000 could be obtained, which is insufficient to detect these extremely small pores.

The plots of the cumulative intrusion and logarithm of the differential intrusion versus pore diameter obtained for the five studied samples are shown in Fig. 3. The observed maximum pore sizes amounted to 4000, 2000, 500, 50, and 30 nm for samples 1, 2, 3, 4, and 5, respectively. Sample 1 contained the widest pore distribution, and its largest peak was centered at 2500 nm (for samples 2, 3, 4, and 5, the largest peaks were detected at 1500, 400, 45, and 20 nm, respectively). As indicated by the plot of the cumulative pore volume (obtained from the cumulated intrusion plotted as a function of the pore size), relatively large pores (>25 nm) accounted for only 20% of the total pore volume. Table 1 also shows that, except for the anomalous total volume of sample 1 (0.17 mL/g) and porosity of sample 3 (36%), the total pore volume gradually decreased from 0.17 to 0.08 mL/g, while the membrane porosity gradually decreased from 51% to 33% with increasing release period. The obtained results indicate that pores with various sizes are characterized by different release rates of nutrients through the membrane. The larger the pore size, the greater are the pore volume and porosity. Therefore, the release period is correspond-

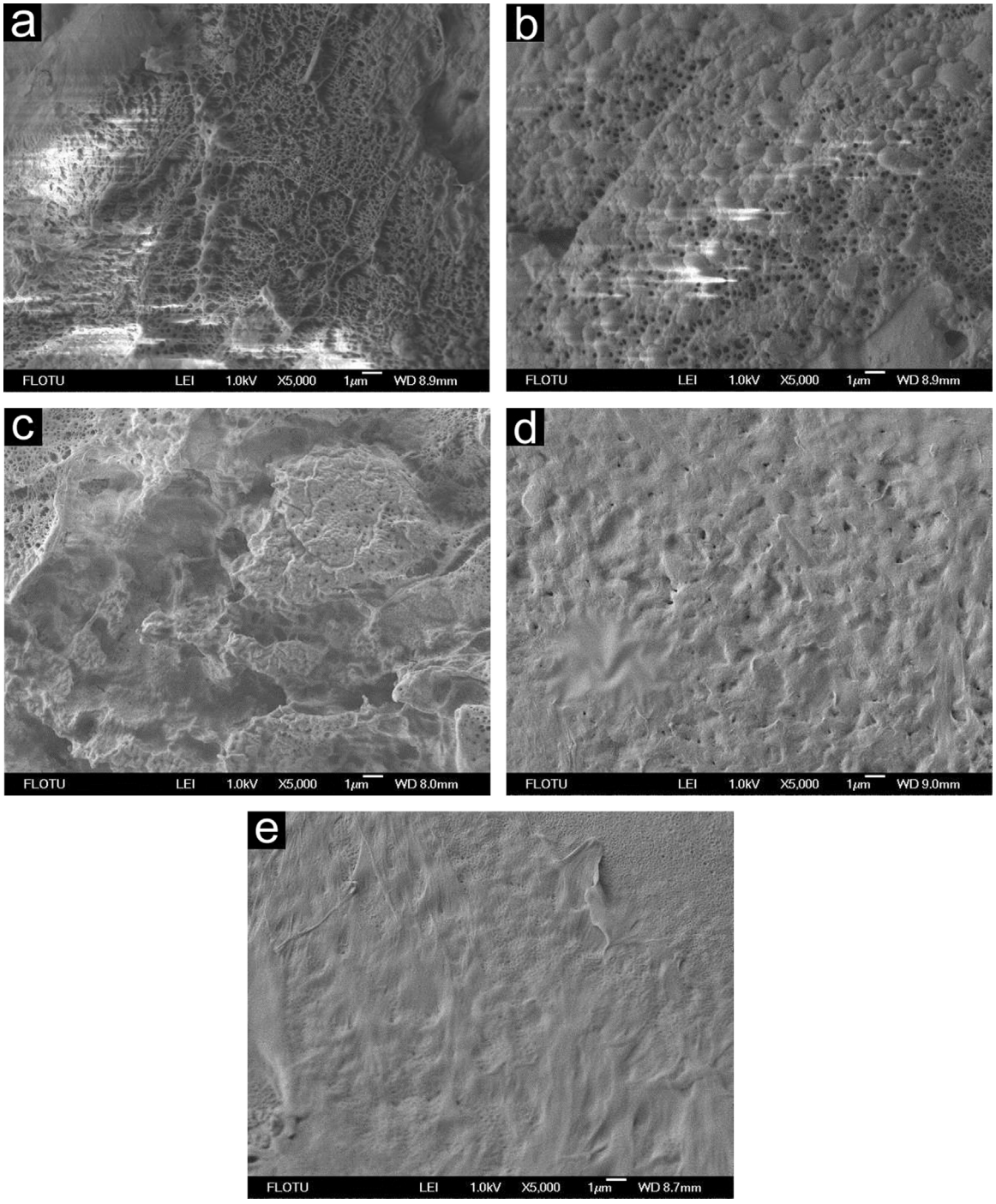

Fig. 2. SEM images of the coated fertilizers with different release durations: (a) sample 1, (b) sample 2, (c) sample 3, (d) sample 4, and (e) sample 5 obtained at a magnification of ×10,000.

ingly shorter. During the phase transformation in the film-forming mechanism, the polymer separates from the solvent phase and forms pores in the film when the separation does not occur rapidly (Mulder, 1996). Yang et al. (2008) showed that differences in the pores arose in response to changing spray conditions: smaller pores were achieved when smaller solvent phase particles were sprayed. However, larger pores were produced when the diameter of the sprayed solvent phase particles increased by 2 times.

In general, the molecular sizes of LDPE, water, and inorganic ions amount to 2–10, 0.2, and 0.2–0.4 nm, respectively (Mulder, 1996). The median pore sizes are in the range of 4.5–5.3 nm, which is very close to the size of PE molecules, suggesting that a relatively large number of membrane pores originated from the gaps between polymer species. According to the definition of the International Union of Pure and Applied Chemistry (Fujita, Takahashi, Ohshima, Ushioda, & Shimizu, 1977), the membrane pores of the tested CRF samples contained both large (greater than 50 nm) and medium (between 2 and 50 nm) pores. The measured pore sizes exceeded the diameter of water molecules (0.2 nm) and mineral ions (0.2–0.4 nm) by a factor of 10, indicating that the latter could freely pass through the membrane pores. The resistance to flow through the pores decreased as pore size increased. Hence, the pores with sizes larger than 25 nm significantly influenced the nutrient release duration from CRFs. Wei et al. (2017) investi-

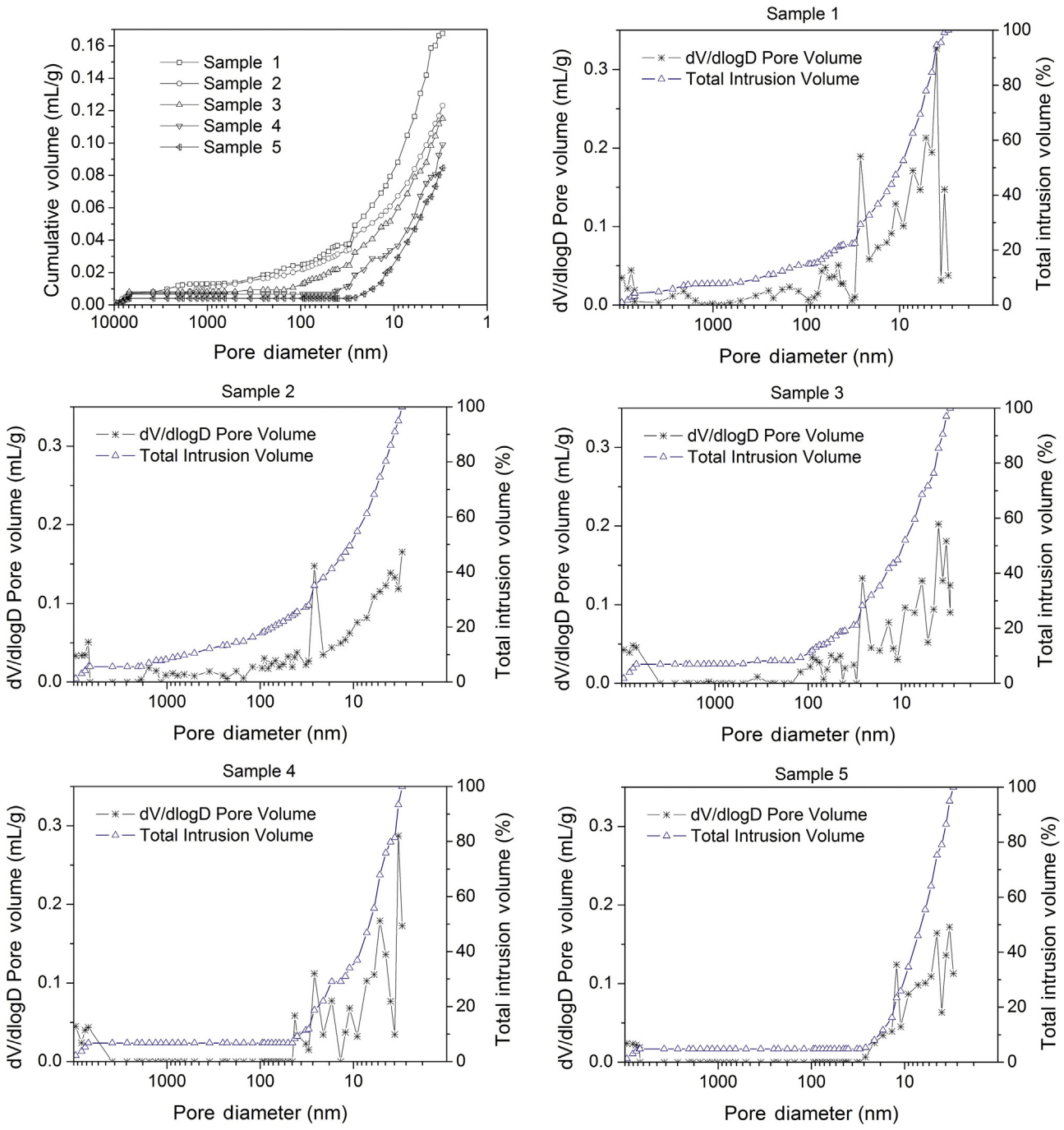

Fig. 3. Relationships between the cumulative pore volumes, differential embedded volumes, and pore diameters of the studied CRF samples.

gated the differences in the permeability coefficient between a PE controlled-release membrane and a dense industrial membrane and concluded that the PE controlled-release film was not a dense membrane but was porous, and that nutrient release is mainly determined by the pore configuration of the membrane.

Modeling nutrient release period

The nutrients steadily diffusing through a uniform pore with length l and radius r can be described by the following equation:

$$J = -D\frac{C_{in} - C_{out}}{l}, \quad (4)$$

where J is the diffusion flux per unit area and per unit time, D is the diffusion coefficient, and C_{in} and C_{out} are the incoming and outgoing nutrient concentrations, respectively. The diffusion rate R can be calculated as

$$R = JA = J\pi r^2. \quad (5)$$

After time t, the released amount of nutrients from the fertilizer to the environment will be

$$N_t = -Rt = D\pi r^2 \frac{C_{in} - C_{out}}{l}. \quad (6)$$

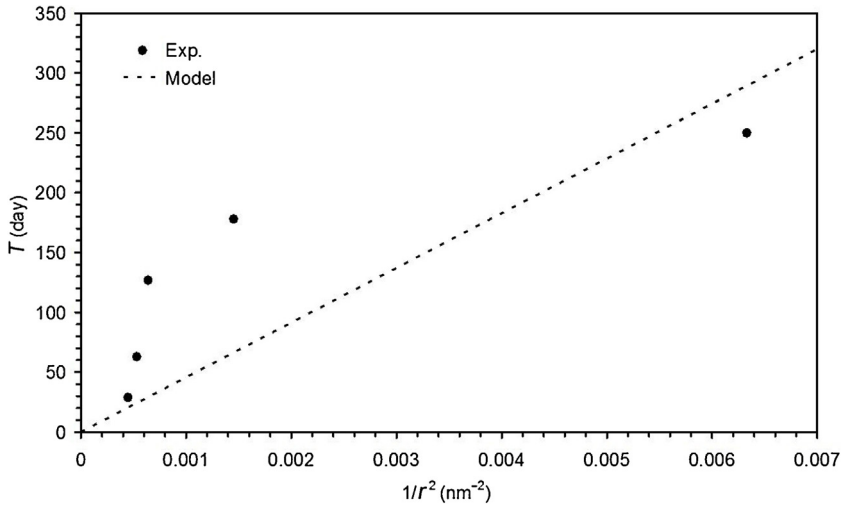

Fig. 4. Comparison of the release periods obtained experimentally and via the model described by Eq. (9) using the average pore sizes. The utilized periods and square radii are taken from Table 1.

Table 2
Dependence of the nutrient release times on the maximum pore diameters.

Sample	1	2	3	4	5	6	7	8	9
Time (day)	29	63	127	178	250	46	105	150	199
D_{eff} (μm)	1.2	0.85	0.53	0.39	0.34	0.93	0.58	0.45	0.41
r^2_{eff} (μm²)	0.360	0.181	0.070	0.039	0.029	0.216	0.084	0.051	0.042

Here, the parameter N is equivalent to the parameter M in Eq. (1). Thus, for a steady diffusion process, $\eta_n \propto r^2$. Without loss of generality, it can be assumed that

$$\eta_1 = k_1 r^2, \eta_{\Delta t} = k r^2, \tag{7}$$

where k_1 and k are the proportionality coefficients. By substituting Eq. (7) to Eq. (3), the following expression can be obtained:

$$T = \frac{K}{r^2} - C. \tag{8}$$

with $K = 0.8/k$ and $C = (k_1 - k)/k$. During stable release, $k = k_1$, and, therefore, $C = 0$. As a result, Eq. (8) can be simplified as follows:

$$T \approx \frac{K}{r^2}, \tag{9}$$

which is reasonable because $T \to 0$ at $r \to \infty$.

Since the actual pore sizes are not uniform, some assumptions have to be made to verify whether Eq. (9) is applicable to the studied CRFs samples. By substituting the average diameter r in Table 1 for the radius in Eq. (9), the corresponding release periods with fitted parameters K were calculated and subsequently compared with the experimental values presented in Fig. 4. The observed large deviations from the experimental results indicate that the utilized assumption was incorrect. Since the largest pores affected the rate of nutrient release most significantly, it was suggested that the effective maximum pore radius would be a better parameter for Eqs. (8) and (9).

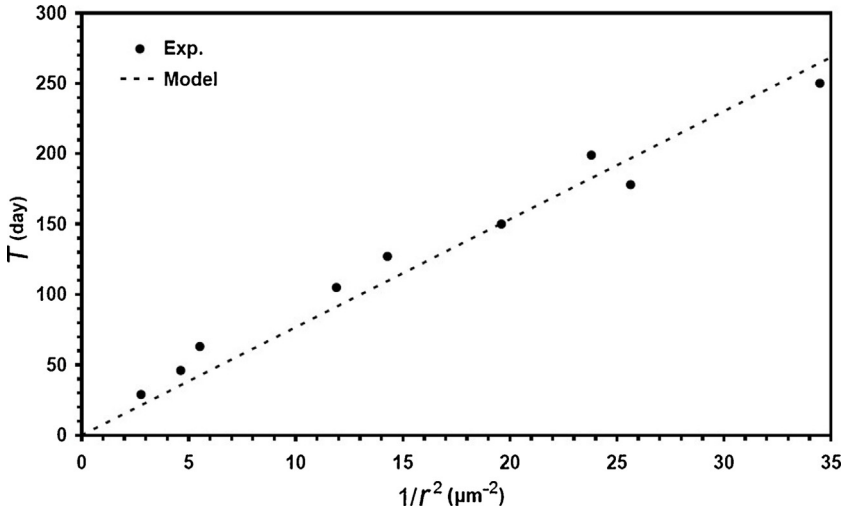

Fig. 5. Comparison of the release periods obtained experimentally and via the model described by Eq. (9) using the effective maximum pore sizes. The periods and square radii are taken from Table 2.

Effective maximum pore diameters

The effective maximum pore diameters (D_{eff}) were determined using the method described in Section 'Pore structure examination' for the five samples specified in Table 1 as well as for four additional samples. The obtained release periods, effective maximum pore diameters, and square radii for the nine tested samples are listed in Table 2.

The experimental release periods presented in Table 2 were fitted with the effective maximum pore sizes using Eq. (9) and then compared with the experimental results displayed in Fig. 5. For the studied samples, the fitted release period can be described by the formula $T = 7.67/r_{eff}^2$, where T is expressed in day, and r_{eff} is expressed in μm. The comparison depicted in Fig. 5 indicates that Eq. (9) can satisfactorily describe the release periods of CRFs. Since the utilized model fitted the experimental data with high accuracy using the effective maximum pore sizes, it can be concluded that the largest membrane pores played the most important role in the nutrient release by CRFs, although they were fewer in number than the smallest pores. In practice, to maintain the high rate of nutrient release over a long period, jamming of the largest pores must be avoided. The described model provides a simple but accurate way to estimate the release period of CRFs by measuring its effective maximum pore size.

Conclusions

Five different types of PE-coated CRFs were fabricated in this work using the spray phase inversion method. The obtained CRFs exhibited steady rates of nutrient release and release periods of 1, 2, 4, 6, and 8 months. Their corresponding cumulative release rates were linearly dependent on the release time, while the release periods strongly correlated with the membrane pore structure. Only relatively large pores were observed in the SEM surface and cross-sectional images.

The membranes of the five studied CRFs exhibited different pore size distributions. The widest distribution contained pores with sizes up to 4000 nm, while the narrowest spanned only up to 30 nm. The nutrient release periods of CRFs were inversely proportional to the ranges of the obtained membrane pore size distributions. A quantitative model was established for the CRFs release period, in which the latter was proportional to the inverse of the square of the effective maximum membrane pore radius. It is possible to predict the release period of a CRFs by measuring only the effective maximum pore size of its membrane using the proposed diffusion model for nutrient release.

Acknowledgements

This work described above was financially supported by National Key R&D Program of China (No. 2017YFD0200703), and the General Program of Natural Science Foundation of China (grant number 31572204). The authors would like to thank Hongying Cai from the Department of Chemical Engineering of Tsinghua University for his help with SEM observations and Dongwu Chang from the Department of Thermal Energy Engineering of Tsinghua University for assistance with MP measurements.

References

Al-Zahrani, S. M. (1999). Controlled release of fertilizers: Modeling and simulation. *International Journal of Engineering Science*, *37*, 1299–1307.

Calvo, J. I., Hernandez, A., Pradanos, P., Martınez, L., & Bowen, W. R. (1995). Pore size distributions in microporous membranes II. Bulk characterization of track-etched filters by air porometry and mercury porosimetry. *Journal of Colloid and Interface Science*, *176*(2), 467–478.

Chu, H., Hosen, Y., & Yagi, K. (2007). NO, N_2O, CH_4 and CO_2 fluxes in winter barley field of Japanese Andisol as affected by N fertilizer management. *Soil Biology and Biochemistry*, *39*(1), 330–339.

Du, C., Zhou, J., Shaviv, A., & Wang, H. (2004). Mathematical model for potassium release from polymer-coated fertiliser. *Biosystems Engineering*, *88*(3), 395–400.

Fujita, T. (1996). Invention of fertilizer coating technology using polyolefin resin and manufacturing of polyolefin coated urea. *Japanese Journal of Soil Science and Plant Nutrition*, *67*(3), 247–248.

Fujita, T., Takahashi, C., Ohshima, M., Ushioda, T., & Shimizu, H. (1977). Method for producing coated fertilizer. *U.S. Patent No. 4019890*.

Hernandez, A., Calvo, J. I., Prádanos, P., Palacio, L., Rodríguez, M. L., & De Saja, J. A. (1997). Surface structure of microporous membranes by computerized SEM image analysis applied to Anopore filters. *Journal of Membrane Science*, *137*(1–2), 89–97.

León y León, C. A. (1998). New perspectives in mercury porosimetry. *Advances in Colloid and Interface Science*, *76*, 341–372.

Liu, F., Du, C. H., Zhu, B. K., & Xu, Y. Y. (2007). Surface immobilization of polymer brushes onto porous poly(vinylidene fluoride) membrane by electron beam to improve the hydrophilicity and fouling resistance. *Polymer*, *48*(10), 2910–2918.

Ma, D., & McHugh, A. J. (2007). The interplay of phase inversion and membrane formation in the drug release characteristics of a membrane-based delivery system. *Journal of Membrane Science*, *298*(1), 156–168.

Mohl, S., & Winter, G. (2004). Continuous release of rh-interferon α-2a from triglyceride matrices. *Journal of Controlled Release*, *97*(1), 67–78.

Mulder, M. (1996). *Basic principles of membrane technology*. Amsterdam: Kluwer Academic Publishers.

Oertli, J. J., & Lunt, O. R. (1962). Controlled release of fertilizer minerals by incapsulating membranes: I. Factors influencing the rate of release. *Soil Science Society of America Journal*, *26*(6), 579–583.

Shavit, U., Reiss, M., & Shaviv, A. (2003). Wetting mechanisms of gel-based controlled-release fertilizers. *Journal of Controlled Release*, *88*(1), 71–83.

Shavit, U., Shaviv, A., & Zaslavsky, D. (1995). Solute diffusion coefficient in the internal medium of a new gel based controlled release fertilizer. *Journal of Controlled Release*, *37*(1–2), 21–32.

Shaviv, A., & Mikkelsen, R. L. (1993). Controlled-release fertilizers to increase efficiency of nutrient use and minimize environmental degradation—A review. *Fertilizer Research*, *35*(1–2), 1–12.

Siepmann, F., Siepmann, J., Walther, M., MacRae, R. J., & Bodmeier, R. (2008). Polymer blends for controlled release coatings. *Journal of Controlled Release*, *125*(1), 1–15.

Sun, Y. M., Huang, W. F., & Chang, C. C. (1999). Spray-coated and solution-cast ethylcellulose pseudolatex membranes. *Journal of Membrane Science*, *157*(2), 159–170.

Trenkel, M. E. (2010). *Slow-and controlled-release and stabilized fertilizers: An option for enhancing nutrient use efficiency in agriculture*. Paris, France: International Fertilizer Industry Association (IFA).

Van de Witte, P., Dijkstra, P. J., Van den Berg, J. W. A., & Feijen, J. (1996). Phase separation processes in polymer solutions in relation to membrane formation. *Journal of Membrane Science*, *117*, 1–31.

Wei, Y., Li, J., Li, Y., Zhao, B., Zhang, L., Yang, X., et al. (2017). Research on permeability coefficient of a polyethylene controlled-release film coating for urea and relevant nutrient release pathways. *Polymer Testing*, *59*, 90–98.

Xu, J. K., Li, X. H., Yang, X. D., Li, Y. T., Li, J., Zhang, J. J., et al. (2016). Study on measuring methods for pore size of polyolefin film coated controlled-release fertilizer. *Journal of Plant Nutrition and Fertilizer*, *22*(3), 794–801 (in Chinese).

Yang, X. D., Cao, Y. P., Jiang, R. F., & Zhang, F. S. (2005). Evaluation of nutrients release feature of coated controlled-release fertilizer. *Plant Nutrition and Fertilizer Science*, *11*(4), 501–507 (in Chinese).

Yang, X., Cao, Y., Jiang, R., Zhang, F., Hu, S., & Guo, B. (2008). Effect of atomization on membrane structure and characteristics during manufacture of polymer-coated controlled-release fertilizer. *Journal of Chemical Industry and Engineering (China)*, *59*(3), 778–784 (in Chinese).